



ELSEVIER

Available online at www.sciencedirect.com



Journal of Colloid and Interface Science ●●● (●●●●) ●●●-●●●

JOURNAL OF
Colloid and
Interface Science

www.elsevier.com/locate/jcis

Sorption of aqueous carbonic, acetic, and oxalic acids onto α -alumina

Cyrille Alliot^{a,*}, Lionel Bion^b, Florence Mercier^b, Pierre Toulhoat^c^a SUBATECH/Ecole des Mines de Nantes, 4 rue Alfred Kastler, BP 20722, 44307 Nantes Cedex 3, France^b UMR 8587 Analyse et Environnement (CEA/CNRS/Université d'Evry Val-d'Essonne), Centre d'Etudes de Saclay, 91191 Gif-sur-Yvette Cedex, France^c CNRS/Université Claude Bernard Lyon 1, UFR de Chimie Biochimie, 43 Bd du 11 Novembre 1918, 69622 Villeurbanne Cedex, France

Received 3 December 2004; accepted 11 February 2005

Abstract

The presence of organic complexing agents can modify the behavior of a surface. This study aims to better understand the impact of carboxylic acids (acetic, oxalic, and carbonic acids) issued from cellulose degradation and equally naturally present in soils. First, evidence of two different kinds of sites for chloride adsorption onto α -alumina and another for sodium sorption was provided. Consequently, no competition between these cation and anion sorptions occurs on α -alumina. The associated exchange capacities and ionic exchange constants were measured. Second, the adsorption behavior of the carboxylic acids was studied as a function of aqueous $-\log[\text{H}^+]$ and 0.01 to 0.1 M ionic strength (NaCl), and modeled by using mass action law for ideal biphasic systems. The carboxylic acids were found to be adsorbed on the same sites as chloride ions. The competition between organic ligands and chloride ions was satisfactorily accounted for by the model assuming the deprotonated form of the ligands was sorbed on α -alumina. The model also allowed us to interpret the adsorption of all species under various conditions without any extra fitting parameters.

© 2005 Elsevier Inc. All rights reserved.

Keywords: Alumina; Acetate; Oxalate; Carbonate; Sorption; Ion-exchange theory

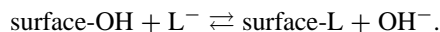
1. Introduction

Sorption of radionuclides on mineral surfaces can considerably delay their migration in groundwaters from a possible waste disposal. However, organic complexing agents could as well be sorbed on solid surfaces, possibly modifying their retention properties for radionuclides. In future nuclear waste management, such modifications can strongly disrupt the behavior of lanthanides or actinides toward natural solids such as oxides and clays: a better understanding of complexing agent adsorption is essential to ensure nuclear waste disposal.

Therefore, the retention of simple carboxylic acids—typically acetic, oxalic, and carbonic acids, which are the ultimate degradation products of cellulose and equally naturally present in soils—is a key phenomenon. These com-

plexing agents can either decrease retention through aqueous complexation and competition for solid surface or increase retention by a synergic effect (adsorption of a metal–ligand complex).

The specific adsorption (partition between aqueous solution and mineral surface) of organic and inorganic compounds on oxides is generally described as ligand exchange reactions [1,2]. The surface OH^- groups are exchanged with L^- , the aqueous anion:



The retention behavior of simple organic acids on a mineral surface is studied here. Metal oxides are often used as a model surface prior to evaluating theories and hypotheses on more complex samples such as clays. Thus, α -alumina was used because of its stability in aqueous solution. Acetic and oxalic acids were chosen because they are ultimate compounds of cellulose degradation and are also released by decay of plant, animal, and microbial tissues [3], and equally because they are model ligands of more complex carboxylic

* Corresponding author. Fax: +33(0)251858452.

E-mail address: cyrille.alliot@subatech.in2p3.fr (C. Alliot).

compound. Aqueous carbonic acid was chosen because of its ubiquitous presence in natural systems: atmosphere studies by aqueous–gaseous phase exchange, dissolution of carbonate minerals, and respiration.

Some studies concerning these carboxylic acids are presented in the literature. All authors agree that a relationship exists between acid–base properties (pK_a) and sorption isotherms. Indeed, adsorption maxima are measured for $pH = pK_a$ in the case of acetate [4], for $pH = pK_{a2}$ in the case of oxalate [5], and for $pH = pK_{a1}$ for carbonate [4]. This adsorption maximum seems to be explained by suitability between complexing agent charge and surface charge. Moreover, all authors observe a competitive effect of chloride in adsorption onto oxide minerals [4,6], meaning that the site for sorption is identical for both. But some uncertainties remain concerning the adsorption mechanisms. If most of them explain their results by ligand exchange mechanism between deprotonated form and surface hydroxide, in the case of oxalic acid and carbonic acid, some authors use only totally deprotonated ligand [7] and others use both deprotonated forms [6].

2. Materials and methods

2.1. Materials

2.1.1. Chemicals and solutions

Alumina (α - Al_2O_3) was purchased from Interchim (pure 99.99%, size fraction 200–500 nm). From pH_{PZNPC} (point zero net proton charge) measurements, we suspected that carbonate ions were sorbed on the surface [8–10]. For this reason, the solid was washed with a carbonate-free 0.1 M aqueous NaOH solution (see below). It was then washed several times with Millipore water until the filtrate was neutral. It was centrifuged, dried, and stored at room temperature in a vacuum desiccator. $pH_{PZNPC} = 9.1$ was measured, indeed corresponding to a carbonate-free surface of alumina [9].

XRD and XPS measurements confirmed that the purified material was still α -alumina, and no impurity was detected (data not shown). A specific surface area of $12 \pm 0.2 \text{ m}^2 \text{ g}^{-1}$ was determined by nitrogen adsorption on the dried powdered alumina.

HCl and NaOH 0.1 M solutions were used to adjust $-\log[H^+]$. They were prepared with Millipore water previously purged with Ar(g). Weighed amounts of 50% NaOH solution, which is carbonate-free because carbonate is not soluble in this solution [11], or 36% HCl solution were added. Carbonate-free NaCl solutions of various concentrations were prepared with weighed Aldrich suprapure NaCl solid. The solutions were spiked with ^{36}Cl or ^{22}Na isotopes (CERCA, 1000 Bq/mL) which did not change the total concentration. The final $-\log[H^+]$ was ca. 7.

Acetate, oxalate, and carbonate solutions were prepared by dissolving weighed amounts of sodium salt (Merck). Sodium chloride was added to obtain a constant ionic

strength. The solutions were spiked with the ^{14}C isotope of the corresponding acid (Amersham International) to obtain a total activity of approximately 380 Bq/mL. The final $-\log[H^+]$ of the oxalate and acetate solutions were approximately 7. For the carbonate solution, the final $-\log[H^+]$ was approximately 10.3, corresponding to a well buffered solution.

2.1.2. Sorption isotherms of Na^+ and Cl^-

A preliminary study allowed us to verify that Na^+ and Cl^- are not significantly adsorbed onto polycarbonate tube walls.

We measured the sorption of Na^+ and Cl^- as a function of $-\log[H^+]$. $[H^+]$ was adjusted with 0.1 M HCl or NaOH aqueous solutions and controlled with a combined pH microelectrode (Mettler Toledo, reference). Its reference cell was filled with NaCl/KCl(sat) and calibrated with solutions of known $[H^+]$, a classic procedure in which activity coefficients and the molal-to-molar conversion factor are constant. This was obtained by working at constant ionic strength: the pH electrode was directly calibrated in $-\log[H^+]$ units. To eliminate the junction potential, all the buffers (acetic acid/acetate 10^{-3} M; carbonic acid/carbonate 10^{-3} M) and working solutions were prepared in media of the same ionic strength controlled by NaCl concentration.

Various amounts of carbonate-free alumina powder were added in 8 mL of various carbonate-free aqueous solutions of various $-\log[H^+]$, $[\text{Na}^+]$, and $[\text{Cl}^-]$. The samples were shaken and centrifuged at 22,000 rpm for 2 h. A 1-mL aliquot of supernatant was analyzed by beta counting for chloride with a Packard Tricarb 2700 liquid scintillator using 4 mL of Ultima Gold scintillant liquid and by gamma counting for sodium with a 1282 Compugamma CS gamma counter. The repartition of $[\text{Na}^+]$ or $[\text{Cl}^-]$ between both phases was deduced from these radiometric analysis of the aqueous phases and from activity balance.

The total concentrations of chloride and sodium were determined by capillary electrophoresis using Quanta 4000 system (Waters). For Cl^- , we used UV-CAT2 as electrolyte, a positive potential, a 30-s hydrostatic injection, and invert UV 185 nm as the detection method. For Na^+ , we used OFM-OH as electrolyte, a negative potential, and invert UV 254 nm as a detection method.

The error bars on the figures were calculated by propagating the uncertainties of masses, counting, and determinations of concentration in solution.

2.1.3. Sorption isotherms of acetate, oxalate, and carbonate

As in the case of Na^+ and Cl^- , a preliminary study did not indicate any adsorption of organic acids onto the tube walls. As for the sodium and chloride isotherms, the sorption of carboxylic acids and carbonate ions was studied as a function of $-\log[H^+]$, but also at different ionic strengths (NaCl). The $-\log[H^+]$ control and the experimental protocol were the same as for the previous study. ^{14}C -spiked ac-

etate, oxalate, and carbonate solutions were used. $-\log[\text{H}^+]$ was adjusted with 0.1 M carbonate-free HCl or NaOH solutions. The sorbed concentration was determined through mass balance.

2.2. Methods

Surface complexation formulas (SCFs) are very popular for interpreting sorption of aqueous cations on oxide and other minerals. However ion-exchange theory (IET) [12,13] can also be used. Both models are able to describe such mechanisms as surface complexation, ion exchange, and any other chemical surface reactions.

However, IET assumes that each phase (the aqueous solution and the solid with the interface) is neutral, while SCF writes only global electroneutrality. SCF also allows several layers for the interface, while IET uses a single chemical potential for each stoichiometry of species at the surface. On the other hand, IET currently assumes several sorption sites, while SCF users seldom do, even though it should be feasible in the framework of SCF. Several sites have to be taken into account when they are evidenced by saturation experiments or physical observations. IET often uses fewer species (hence fewer fitted parameters) with stoichiometries restricted by the interface electroneutrality condition. No explicit electrostatic term is included in IET, as for mass action law in the bulk solution. Consequently stoichiometric coefficients are obtained by classic slope analysis of \log - \log plots for IET, which is a way of checking the model. For this reason, we used constant ionic strength for each set of experiments, as classically done in solution chemistry leading to equilibrium constants for each ionic strength; these equilibrium constants appeared to have the same numerical values in the ionic strength range used in this study within experimental uncertainties and using activity coefficients only for the bulk aqueous species. This indicates negligible influence of the activity coefficients for the sorbed species (or their influences cancel out) within the framework of IET, while for SCF this indicates negligible variations of the electrostatic terms, or their compensation by the activity coefficients. For these reasons we treated our data with IET. As a consistent model could be proposed, we did not attempt to test SCF.

The system includes two totally nonmiscible and electrically neutral phases: a solid phase—actually its surface with a few layers of water—named ion exchange, and a liquid phase—an aqueous solution that exchanges ions with the solid phase. The charges of the surface are exactly compensated by ions coming from the aqueous solution.

No postulate limits the number of different sites, which have an exchange capacity to be measured by typical saturation experiments, when feasible.

2.2.1. Cationic salt adsorption

When the sorption of a cation is observed, it is explained as an exchange between H^+ ions of the surface and M^+

aqueous cationic ions,



where $\{\equiv\text{Al}_i\text{X}\}$ is species X adsorbed on site i of the surface. The selectivity coefficient of Eq. (1) is

$$K_{\text{M}/\text{H}}^{*i} = \frac{[\{\equiv\text{Al}_i\text{OH}\}][\text{M}^+]_{\gamma_{\text{M}}}}{[\{\equiv\text{Al}_i\text{O}^-\text{M}^+\}][\text{H}^+]_{\gamma_{\text{H}}}}, \quad (2)$$

where $[\text{X}]$ is the aqueous concentration of X; $\{\text{X}\}$, the concentration of X adsorbed species; γ , the activity coefficient of aqueous species. The activity coefficients of adsorbed species are included in the equilibrium constant. The activity coefficients of aqueous species are calculated with the Davies equation. They actually cancel out because M^+ and H^+ have the same charge. Moreover, considering the mass balance

$$[\{\equiv\text{Al}_i\text{O}^-\text{M}^+\}] = \frac{\text{Ce}_i}{1 + \frac{K_{\text{M}/\text{H}}^{*i}[\text{H}^+]_{\gamma_{\text{H}}}}{[\text{M}^+]_{\gamma_{\text{M}}}}}, \quad (3)$$

where Ce_i is the exchange capacity site i concerned by sorption.

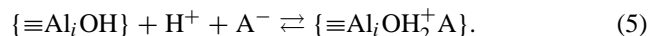
$[\text{M}^+]$ was measured by capillary electrophoresis, and pH was also measured. To compare experimental data and to model them whatever the salt concentration, a variable modification is used: $X = \log(a(\text{Na}^+)/a(\text{H}^+))$. So the concentration of M adsorbed on a site i is

$$[\{\equiv\text{Al}_i\text{O}^-\text{M}^+\}] = \frac{\text{Ce}_i}{1 + \frac{K_{\text{M}/\text{H}}^{*i}}{10^X}} = \frac{\text{Ce}_i}{1 + 10^{\log(K_{\text{M}/\text{H}}^{*i}) - X}}. \quad (4)$$

The exchange capacities and associated selectivity coefficients were determined by curve fitting. To model experimental data, the least possible number of sites was used. This model can be verified by an analysis slope of $\log\{\text{Al}_i\text{O}^-\text{M}^+\} = f(X)$ representation. If the site is principally under $\{\text{Al}_i\text{OH}\}$ form, we can measure a slope equal to one. But if $\{\text{Al}_i\text{O}^-\text{Na}^+\}$ is majority, the curve presents a plateau equal to $\log \text{Ce}_i$.

2.2.2. Anionic salt adsorption

The adsorption of an anionic salt was written as the neutralization for the adsorption of H^+ in acid media:



The selectivity coefficient is defined as

$$K_{\text{A}}^{*i} = \frac{[\{\equiv\text{Al}_i\text{OH}_2^+\text{A}^-\}]}{[\{\equiv\text{Al}_i\text{OH}\}][\text{H}^+][\text{A}^-]_{\gamma_{\text{H}}\gamma_{\text{A}}}}. \quad (6)$$

The dehydration reaction $\{\equiv\text{Al}_i\text{OH}_2^+\text{A}^-\} \rightarrow \{\equiv\text{Al}_i\text{A}\} + \text{H}_2\text{O}$ is not likely, and anyway would lead to formally the same equations since the activity of water is constant. As for cationic salt adsorption, the mass balance was used to obtain

$$[\{\equiv\text{Al}_i\text{OH}_2^+\text{A}^-\}] = \frac{\text{Ce}_i}{1 + \frac{1}{K_{\text{A}}^{*i}[\text{H}^+][\text{A}^-]_{\gamma_{\text{H}}\gamma_{\text{A}}}}}. \quad (7)$$

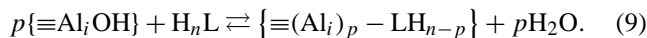
$-\log[\text{H}^+]$ was measured, and the concentration of anionic salt was determined by capillary electrophoresis. As in the case of sorption of cationic salt, a variable modification is used to represent experimental data: $X = -\log(a(\text{H}^+) \times a(\text{Cl}^-))$ to consider as anionic salt effect. So the concentration of adsorbed anionic salt on site i is

$$[\{\equiv\text{Al}_i\text{OH}_2^+\text{A}^-\}] = \frac{\text{Ce}_i}{1 + \frac{10^X}{K_A^{*i}}} = \frac{\text{Ce}_i}{1 + 10^{\log(-K_A^{*i}) + X}}. \quad (8)$$

As for cationic salt adsorption, we can represent anionic salt adsorption with a bilogarithmic curve $\log[\text{A}^-]_{\text{ads}} = f(X)$. In more acidic media—maximum anionic salt adsorption—the curve presents a slope equal to $\log \text{Ce}_i$. When acidity diminishes, we must observe a slope equal to 1, corresponding to desorption of anionic salt.

2.2.3. Carboxylic acid adsorption

Sorption of carboxylic acid was written as the result of a ligand exchange mechanism:



The activity coefficient of neutral species was set at 1:

$$K_{\text{LH}_{n-p}}^{*i} = \frac{[\{\equiv(\text{Al}_i)_p\text{LH}_{n-p}\}]a_{\text{H}_2\text{O}}^p}{[\{\equiv\text{Al}_i\text{OH}\}]^p[\text{H}_n\text{L}]}. \quad (10)$$

The mass balance on site i , concerned by sorption, is

$$\text{Ce}_i = [\{\equiv\text{Al}_i\text{OH}\}] + [\{\equiv\text{Al}_i\text{OH}_2^+\text{A}^-\}] + [\{\equiv\text{Al}_i\text{O}^-\text{M}^+\}] + \sum_{p=1}^n p[\{\equiv(\text{Al}_i)_p\text{LH}_{n-p}\}]. \quad (11)$$

With appropriate selectivity coefficients and other parameters, $[\{\text{Al}_i\text{OH}\}]$ can be simply explained for the adsorption of a diacid H_2L :

$$\begin{aligned} \text{Ce}_i &= [\{\text{Al}_i\text{OH}\}] + [\{\text{Al}_i\text{OH}\}]K_{\text{A}}a(\text{H}^+)a(\text{A}^-) \\ &+ [\{\text{Al}_i\text{OH}\}]K_{\text{M}/\text{H}}\frac{a(\text{H}^+)}{a(\text{M}^+)} \\ &+ \sum_{p=1}^n \left(K_{\text{LH}_{n-p}}^{*i} [\{\text{Al}_i\text{OH}\}]^p \frac{[\text{H}_n\text{L}]}{a(\text{H}_2\text{O})^p} \right). \end{aligned} \quad (12)$$

So the total concentration of adsorbed carboxylic acid ($[\{\text{L}\}]$) is

$$[\{\text{L}\}] = \sum_i \left(K_{\text{LH}}^{*i} [\{\text{Al}_i\text{OH}\}] \frac{[\text{H}_2\text{L}]}{a(\text{H}_2\text{O})} + K_{\text{L}}^{*i} [\{\text{Al}_i\text{OH}\}] \frac{[\text{H}_2\text{L}]}{a(\text{H}_2\text{O})^2} \right). \quad (13)$$

If the ligand is a monoacid, $[\{\text{Al}_i\text{OH}\}]$ is written as

$$[\{\text{Al}_i\text{OH}\}] = \frac{\text{Ce}_i}{(1 + K_{\text{A}}a(\text{H}^+)a(\text{A}^-) + K_{\text{M}/\text{H}}\frac{a(\text{H}^+)}{a(\text{M}^+)} + K_{\text{L}}\frac{[\text{HL}]}{a(\text{H}_2\text{O})})} \quad (14)$$

Table 1

Acid–base properties of carboxylic acids [17–20]

Equilibrium	$\log K$
$\text{H}_2\text{O} + \text{CO}_2(\text{aq}) \rightleftharpoons \text{HCO}_3^- + \text{H}^+$	-6.349 ± 0.005
$\text{HCO}_3^- \rightleftharpoons \text{CO}_3^{2-} + \text{H}^+$	-10.337 ± 0.003
$\text{H}_2\text{C}_2\text{O}_4 \rightleftharpoons \text{HC}_2\text{O}_4^- + \text{H}^+$	-1.401 ± 0.052
$\text{HC}_2\text{O}_4^- \rightleftharpoons \text{C}_2\text{O}_4^{2-} + \text{H}^+$	-4.264 ± 0.014
$\text{CH}_3\text{COOH} \rightleftharpoons \text{CH}_3\text{COO}^- + \text{H}^+$	-4.757 ± 0.002

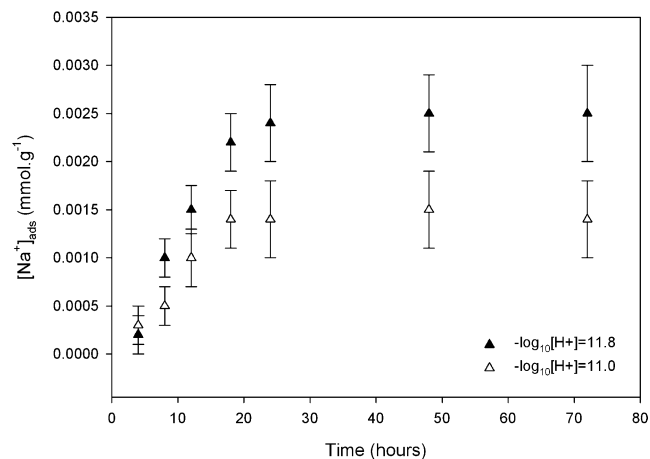


Fig. 1. Sodium sorption for 10 g/L alumina suspension in 0.001 M NaCl as a function of time.

and

$$[\{\text{L}\}] = \sum_i \left(K_{\text{L}}^{*i} [\{\text{Al}_i\text{OH}\}] \frac{[\text{HL}]}{a(\text{H}_2\text{O})} \right). \quad (15)$$

The concentration of adsorbed ligand was calculated as the sum of its concentrations on all sites i . The concentration of H_nL was calculated from the total aqueous concentration of ligand L determined by isotopic dilution principle and its acid–base properties (Table 1).

3. Results and discussions

3.1. Sorption of Na^+

3.1.1. Kinetic and reversibility studies

The time needed to achieve equilibrium was first determined, and the reversibility of adsorption was checked (Fig. 1). Forty-eight hours was long enough to obtain equilibrium conditions. Consequently, the batches were shaken for 3 days. To check the reversibility of sorption, the equilibrium $-\log[\text{H}^+]$ was attained in two different ways. As the same results were obtained in both cases, the system was considered reversible. Consequently, sodium sorption can be modeled by thermodynamics.

3.1.2. Sorption isotherm of sodium

The results of the ^{22}Na adsorption experiments are illustrated in Fig. 2, where sodium concentration is variable due

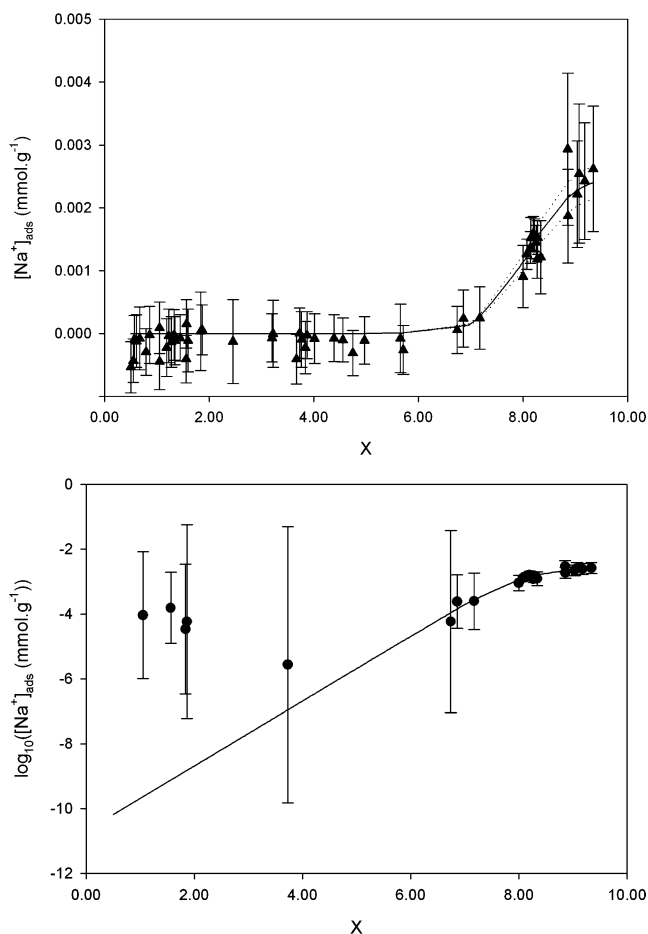


Fig. 2. Sodium sorption on alumina, as a function of $X = -\log[H^+] + \log(a(Na^+)/\gamma(H^+))$. The curve (solid line) was calculated assuming Na^+/H^+ ionic exchange on a single site (Table 2) and corresponding uncertainty on the equilibrium constant (dashed line).

to $-\log[H^+]$ adjustment (NaOH additions also contributed to the initial Na concentration). The activity coefficients of aqueous species were calculated with the Davies equation. The error bars were calculated by propagating all the experimental uncertainties. Negative adsorptions, which are not represented in Fig. 2b, are due to errors on mass balance. The deviation between experimental results and fitted curve for $X < 4$ are equally due to errors on mass balance. No sorption was detected for $X < 6$, while Na^+ sorption increased with X for $X > 7$. Consequently, sodium does not interact with alumina in acidic media.

As sodium sorption is observed for $-\log[H^+] > 9.1$, the point of zero charge, this sorption is certainly the consequence of a compensation of surface charge. Concerning an eventual charge exclusion effect (alumina surface charge electrostatically drives off ions and so forbids them a solution volume), drawing by negative sorption, observed generally in acid media for sodium adsorption, no conclusion can be drawn from the experimental data because of errors associated with experimental points. Knowing the surface area of alumina determined by N_2 -BET, an exchange capacity of $0.25 \mu\text{mol m}^{-2}$ is calculated, which is of the same size order

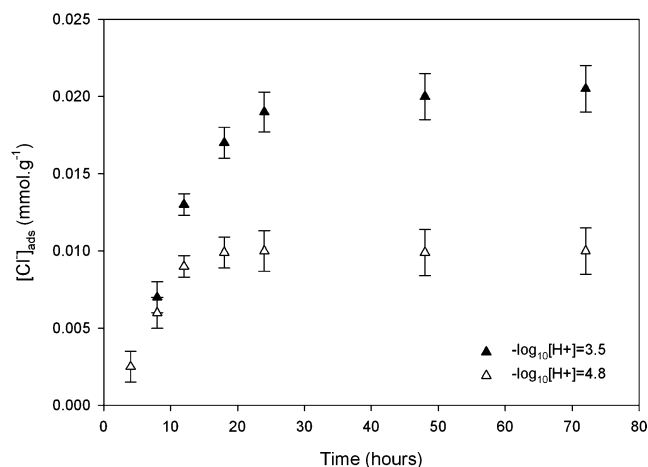


Fig. 3. Chloride sorption for 10 g/L alumina suspension in 0.01 M NaCl as a function of time.

as that of Rundberg et al. [14], who obtained $0.5 \mu\text{mol m}^{-2}$ for goethite, which has a point of zero charge equal to 8.4.

To model experimental results, using a unique site was sufficient (Fig. 2). The associated uncertainties were from the fit using the Microsoft Excel macro proposed by De Levie [15]. The variances in exchange capacity and apparent thermodynamic constant allowed calculation of the associated errors of fit by error propagation.

3.2. Sorption of Cl^-

3.2.1. Kinetic and reversibility studies

As in the case of sodium, the reversibility of chloride sorption was verified and the time needed to achieve of equilibrium conditions was determined. The experimental protocols were similar to those for Na^+ . However, 3 days were needed to obtain equilibrium conditions (see Fig. 3, where the error bars were calculated by propagating the uncertainties of masses, counting, and determinations of concentrations in solution). Moreover the sorption is reversible. Thus, thermodynamics can be used to model the experimental data.

3.2.2. Sorption isotherms of chloride

The results of ^{36}Cl sorption are illustrated in Fig. 4 where chloride concentration varied as a result of $-\log[H^+]$ adjustments (HCl additions also contribute to the initial Cl concentrations). The activity coefficients were calculated with the Davies equation. The error bars were calculated by propagating the experimental uncertainties. Negative chloride adsorptions are treated as for sodium. Sorption increases with aqueous acidity, and is not detected for $X > 9$. So, as for sodium, chloride sorption results in surface charge compensation. Once again, charge exclusion effect in basic media was not observed: the lack of experimental data and the errors bars associated did not allow any clear conclusions to be drawn.

Schulthess and McCarthy [4] studied chloride sorption on aluminum oxide. They obtained an exchange capacity of

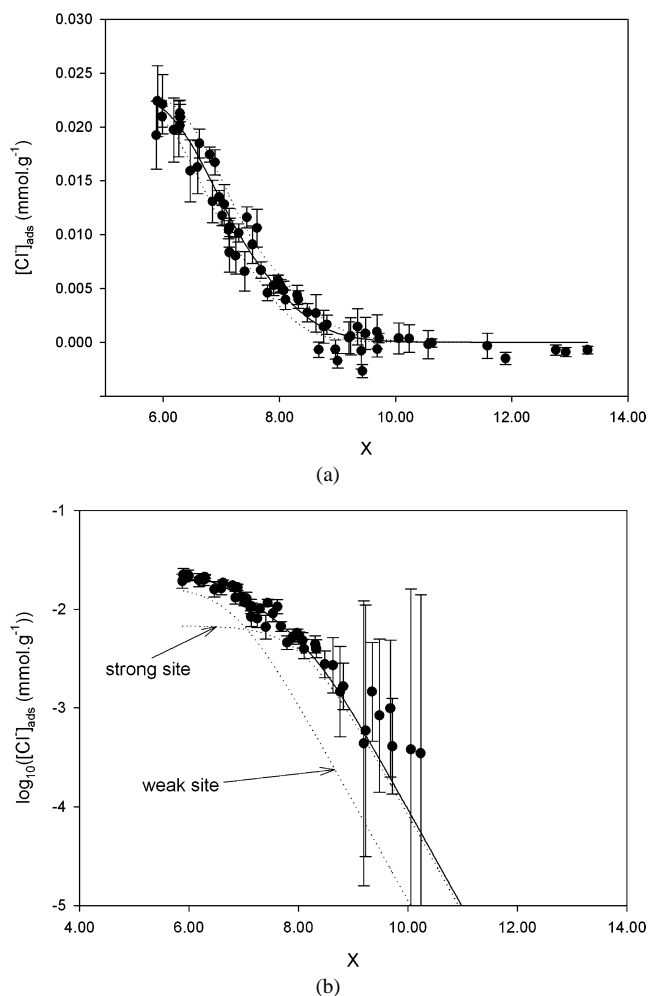


Fig. 4. Chloride sorption by α -alumina as a function of $-\log[H^+] - \log(a(Cl^-)\gamma(H^+))$. (b) The contributions of two different sites are represented by the dashed lines. The curve (solid line) was calculated assuming Na^+/H^+ ionic exchange on a single site (Table 2) and corresponding uncertainty on the equilibrium constant (dashed line).

approximately $2 \mu mol$ per square meter in NaCl medium. Considering the specific surface area of alumina, we also obtained approximately $2 \mu mol m^{-2}$. Consequently, our results are in agreement with those of Schulthess and McCarthy [4].

Two distinct sorption sites were now needed to model our experimental observations. The parameters obtained are listed in Table 2 with their associated uncertainties.

In conclusion three different sites on corundum are needed to model our experimental data: two sites of weak base type, and one of weak acid type.

3.3. Sorption of acetic acid

3.3.1. Kinetic and reversibility studies

From the time needed to obtain equilibrium (see Fig. 5 where the error bars were calculated by propagating the uncertainties of masses, counting, and determinations of concentrations in solution), a shaking time of 4 days was chosen and the reversibility of acetate adsorption checked.

3.3.2. Sorption isotherms of acetate

Fig. 6 represents acetate sorption on α -alumina. NaCl concentration was varied to evidence competitive adsorption between chloride and acetate: the presence of NaCl indeed affects acetate adsorption. The activity coefficients were calculated with the Davies equation. The error bars were calculated by propagating the experimental uncertainties. According to the results presented in Fig. 4, which shows chloride adsorption, the desorption of acetate can be interpreted as the result of competitive chloride adsorption.

The maximum uptake of acetate is observed for $-\log[H^+] = pK_a$. This has already been shown on γ -alumina [4,16], and has been explained by the preferential sorption of the deprotonated form of acetic acid. Consequently, we model our experimental data, as the sorption of the deprotonated form of acetic acid on the same sites as already determined for chloride adsorption (Table 2). This gives confidence in the model: no new fitted exchange capacity was needed to describe the sorption of a new species, i.e., acetic acid.

The parameters used to model the experimental data are listed in Table 2. It is important to note that all parameters are obtained by simultaneously modeling results on chloride, sodium, and acetate sorption. It is the reason why the model obtained for acetate sorption in 0.05 M NaCl medium seems to be perfectible (Fig. 6).

3.4. Sorption of oxalic acid

Three days were needed to obtain sorption equilibrium. Fig. 7 represents oxalate adsorption on alumina, where the activity coefficients were calculated with the Davies equation, and the error bars were calculated by propagating the experimental uncertainties. This figure presents only the $-\log[H^+]$ effect on adsorption. According to this sorption isotherm, oxalate affinity is of the same order of magnitude as acetate affinity. The ratio, equal to 2, between the maximum quantities of sorbed ligand in both cases can be explained by charges of the adsorbed species. Indeed, above $-\log[H^+] 4$, the oxalate is a dianion. This suggests that the mechanism of sorption is likely bidentate (i.e., two aluminol groups are bound to one oxalate).

The results are not in good agreement with those of Violante et al. [5] on aluminum oxide, except for the adsorption maximum: Violante et al. obtain $700 \mu mol g^{-1}$, and we obtained $10 \mu mol/g$. However, the solid used by Violante et al. was amorphous; thus its reactivity is more important (specific surface of $120 m^2/g$).

This ligand is a diacid. So, two reactions are considered to model experimental data: a monodentate adsorption and a bidentate adsorption. To test this hypothesis, the least possible reactions are used to model all experimental data. The IET is used with the parameters already determined for sodium and chloride sorptions (Table 2). There is good agreement between experimental data and the model. Sorption of oxalate on α -alumina can be modeled only by taking

Table 2

Formation constants of species considered in modeling the alumina surface: sodium, chloride, acetate, oxalate, and carbonate sorption

Na ⁺ and Cl ⁻ sorption			
$\{\equiv\text{Al}_i\text{O}^-\text{Na}^+\} + \text{H}^+ \rightleftharpoons \{\equiv\text{Al}_i\text{OH}\} + \text{Na}^+$	$K_{\text{Na}/\text{H}}^{*i} = \frac{[\{\equiv\text{Al}_i\text{OH}\}][\text{Na}^+]_{\text{M}}}{[\{\equiv\text{Al}_i\text{O}^-\text{Na}^+\}][\text{H}^+]_{\text{H}}}$	$\text{Ce}_i = 2.5 \pm 0.1 \mu\text{mol/g}$	$\log K_{\text{Na}/\text{H}}^{*i} = 8.09 \pm 0.03$
$\{\equiv\text{Al}_j\text{OH}\} + \text{H}^+ + \text{Cl}^- \rightleftharpoons \{\equiv\text{Al}_j\text{OH}_2^+\text{Cl}^-\}$	$K_{\text{Cl}}^{*j} = \frac{[\{\equiv\text{Al}_j\text{OH}_2^+\text{Cl}^-\}]}{[\{\equiv\text{Al}_j\text{OH}\}][\text{H}^+][\text{Cl}^-]_{\text{H}}\gamma_{\text{Cl}}}$	$\text{Ce}_j = 6.8 \pm 3.5 \mu\text{mol/g}$	$\log K_{\text{Cl}}^{*j} = 8.09 \pm 0.35$
$\{\equiv\text{Al}_k\text{OH}\} + \text{H}^+ + \text{Cl}^- \rightleftharpoons \{\equiv\text{Al}_k\text{OH}_2^+\text{Cl}^-\}$	$K_{\text{Cl}}^{*k} = \frac{[\{\equiv\text{Al}_k\text{OH}_2^+\text{Cl}^-\}]}{[\{\equiv\text{Al}_k\text{OH}\}][\text{H}^+][\text{Cl}^-]_{\text{H}}\gamma_{\text{Cl}}}$	$\text{Ce}_k = 17.2 \pm 2.3 \mu\text{mol/g}$	$\log K_{\text{Cl}}^{*k} = 6.81 \pm 0.21$
Acetate sorption			
$\{\equiv\text{Al}_j\text{OH}\} + \text{AcOH} \rightleftharpoons \{\equiv\text{Al}_j\text{-OAc}\} + \text{H}_2\text{O}$	$K_{\text{Ac}}^{*j} = \frac{[\{\equiv\text{Al}_j\text{-OAc}\}]\alpha(\text{H}_2\text{O})}{[\{\equiv\text{Al}_j\text{OH}\}][\text{AcOH}]}$	$\text{Ce}_j = 6.8 \pm 3.5 \mu\text{mol/g}$	$\log K_{\text{Ac}}^{*j} = 5.71 \pm 0.55$
$\{\equiv\text{Al}_k\text{OH}\} + \text{AcOH} \rightleftharpoons \{\equiv\text{Al}_k\text{-OAc}\} + \text{H}_2\text{O}$	$K_{\text{Ac}}^{*k} = \frac{[\{\equiv\text{Al}_k\text{-OAc}\}]\alpha(\text{H}_2\text{O})}{[\{\equiv\text{Al}_k\text{OH}\}][\text{AcOH}]}$	$\text{Ce}_k = 17.2 \pm 2.3 \mu\text{mol/g}$	$\log K_{\text{Ac}}^{*k} = 4.07 \pm 0.16$
Oxalate sorption			
$2\{\equiv\text{Al}_j\text{OH}\} + \text{H}_2\text{Ox} \rightleftharpoons \{\equiv\text{Al}_{j2}\text{-Ox}\} + 2\text{H}_2\text{O}$	$K_{\text{Ox}}^{*j} = \frac{[\{\equiv\text{Al}_{j2}\text{-Ox}\}]\alpha(\text{H}_2\text{O})^2}{[\{\equiv\text{Al}_j\text{OH}\}]^2[\text{H}_2\text{Ox}]}$	$\text{Ce}_j = 6.8 \pm 3.5 \mu\text{mol/g}$	$\log K_{\text{Ox}}^{*j} = 14.69 \pm 0.22$
$2\{\equiv\text{Al}_k\text{OH}\} + \text{H}_2\text{Ox} \rightleftharpoons \{\equiv\text{Al}_{k2}\text{-Ox}\} + 2\text{H}_2\text{O}$	$K_{\text{Ox}}^{*k} = \frac{[\{\equiv\text{Al}_{k2}\text{-Ox}\}]\alpha(\text{H}_2\text{O})^2}{[\{\equiv\text{Al}_k\text{OH}\}]^2[\text{H}_2\text{Ox}]}$	$\text{Ce}_k = 17.2 \pm 2.3 \mu\text{mol/g}$	$\log K_{\text{Ox}}^{*k} = 12.02 \pm 0.08$
Carbonate sorption			
$2\{\equiv\text{Al}_j\text{OH}\} + \text{H}_2\text{CO}_3 \rightleftharpoons \{\equiv\text{Al}_{j2}\text{-CO}_3\} + 2\text{H}_2\text{O}$	$K_{\text{CO}_3}^{*j} = \frac{[\{\equiv\text{Al}_{j2}\text{-CO}_3\}]\alpha(\text{H}_2\text{O})^2}{[\{\equiv\text{Al}_j\text{OH}\}]^2[\text{H}_2\text{CO}_3]}$	$\text{Ce}_j = 6.8 \pm 3.5 \mu\text{mol/g}$	$\log K_{\text{CO}_3}^{*j} = 11.35 \pm 0.53$
$2\{\equiv\text{Al}_k\text{OH}\} + \text{H}_2\text{CO}_3 \rightleftharpoons \{\equiv\text{Al}_{k2}\text{-CO}_3\} + 2\text{H}_2\text{O}$	$K_{\text{CO}_3}^{*k} = \frac{[\{\equiv\text{Al}_{k2}\text{-CO}_3\}]\alpha(\text{H}_2\text{O})^2}{[\{\equiv\text{Al}_k\text{OH}\}]^2[\text{H}_2\text{CO}_3]}$	$\text{Ce}_k = 17.2 \pm 2.3 \mu\text{mol/g}$	$\log K_{\text{CO}_3}^{*k} = 6.19 \pm 0.12$

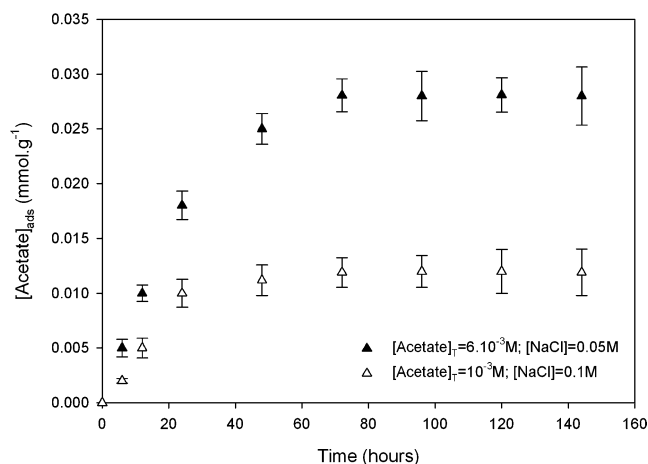


Fig. 5. Acetate sorption for 10 g/L suspension of alumina as a function of time ($-\log[\text{H}^+] = 4.8$).

a bidentate mechanism and the concerned sites are the same as those determined for acetate and chloride. This again provides confidence in the model: no new fitted exchange capacity was needed to describe the sorption of a new species, i.e., oxalic acid.

3.5. Sorption of carbonic acid

The last ligand studied was carbonic acid. An important difference from oxalic acid was in the experimental protocol: while it was easy to control the total concentration of oxalic acid in the system, it is more difficult to control the total concentration of carbonate, as it can be exchanged with CO₂(g) in the air. For this reason, the effect of $-\log[\text{H}^+]$ on carbonate sorption was studied only for $-\log[\text{H}^+]$ values greater than 7. Fig. 8 represents the effect of $-\log[\text{H}^+]$ and ionic

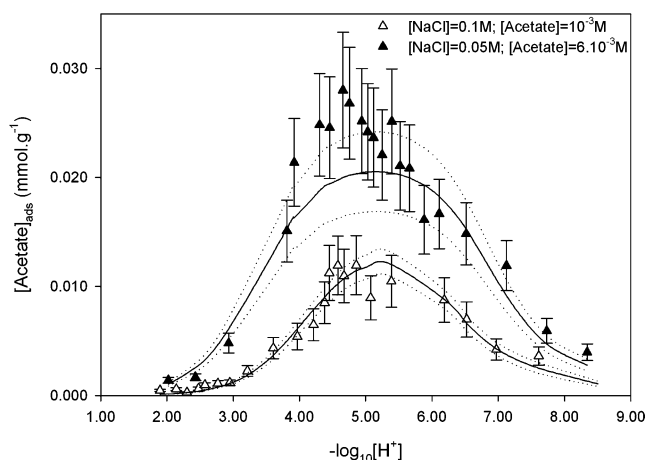


Fig. 6. Effect of $-\log[\text{H}^+]$ and NaCl concentration on acetate sorption by α -alumina 10 g/L. The curve (solid line) was calculated assuming chloride and acetate adsorption on two sites previously determined (Table 2) and corresponding uncertainty on the equilibrium constant (dashed line).

strength (NaCl) on carbonate sorption on α -alumina: the adsorption decrease when $-\log[\text{H}^+]$ increases. But in acidic media, the sorption would also have to decrease because of the lack of species that can sorb on α -alumina.

Experimental data are in good agreement with those obtained by Schulthess et al. [4]. Indeed, a maximum value of adsorption equal to 12 $\mu\text{mol g}^{-1}$ or 1 $\mu\text{mol m}^{-2}$ is near the value of 0.6 $\mu\text{mol m}^{-2}$ determined by Schulthess and McCarthy.

The parameters of the fit are listed in Table 2. The monodentate mechanism is not necessary to model experimental data. But it would be interesting to perform a study in a more acidic medium to confirm this point. Indeed, hydrogenocarbonate is dominating in more acidic media, and if the sorption reaction exists, it will also be dominating.

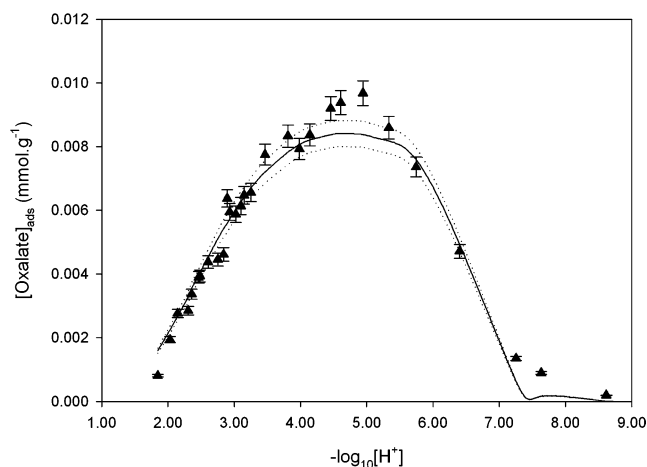


Fig. 7. Effect of $-\log[H^+]$ on oxalate sorption by α -alumina 10 g/L. The curve (solid line) was calculated assuming chloride and oxalate adsorption on two sites previously determined (Table 2) and corresponding uncertainty on the equilibrium constant (dashed line).

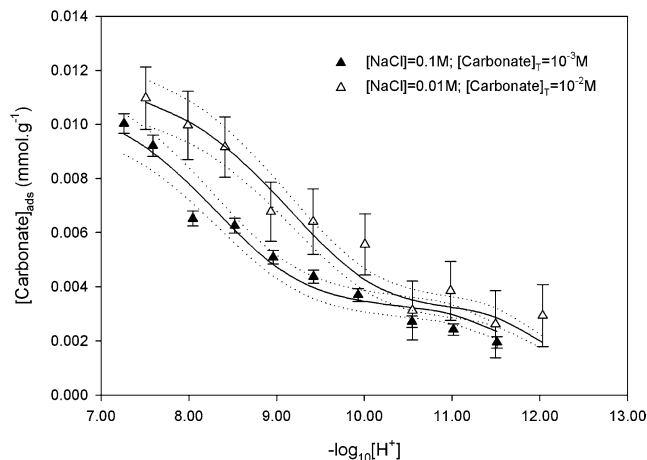


Fig. 8. Effect of $-\log[H^+]$ and NaCl concentration on carbonate sorption by α -alumina 35 g/L. The curve (solid line) was calculated assuming chloride and carbonate adsorption on two sites previously determined (Table 2) and corresponding uncertainty on the equilibrium constant (dashed line).

4. Summary

All experimental data were modeled with a quite restricted set of parameters: typically a restricted number of sorption sites was enough to model the sorption of various organic acids. Thus the model can predict acetate, oxalate, and carbonate behavior in NaCl media on α -alumina with the totally deprotonated form of carboxylic acid.

The thermodynamic constants, i.e., selectivity coefficients (Table 2), are related to ionic media, where they were

measured, because the effects of activity coefficients are classically obtained (by empirical formula and tabulated parameters, or measured) only in bulk aqueous solutions, but not on solid phases. Consequently, the model can be used in media of 0 to 0.1 M ionic strength (allowing use of most of the Debye–Hückel-derived models). Beyond this concentration, one may consider the possible effect of activity coefficients on sorption sites.

As all acids are adsorbed on alumina, we now have the starting point needed for studying more complicated systems as obtained by adding radionuclides.

Acknowledgments

The authors thank Dr. J. Ly, Dr. I. Pointeau, Dr. P. Reiller, and Dr. P. Vitorge for useful conversations.

References

- [1] W. Stumm, R. Kummert, L. Sigg, *Croat. Chem. Acta* 53 (1980).
- [2] W. Stumm, *Geoderma* 38 (1986) 19.
- [3] A. Rovira, *Bot. Rev.* 35 (1969) 35.
- [4] C. Schulthess, J. McCarthy, *Soil Sci. Am. J.* 54 (1990) 688.
- [5] A. Violante, M. Rao, A. De Chiara, L. Gianfreda, *Eur. J. Soil Sci.* 47 (1996) 241.
- [6] K. Mesuere, W. Fish, *Environ. Sci. Technol.* 26 (1992) 2365.
- [7] N. Kallay, E. Matijevic, *Langmuir* 1 (1985) 195.
- [8] A. Van Geen, A. Robertson, J. Leckie, *Geochim. Cosmochim. Acta* 58 (1994) 2073.
- [9] E. Scholtz, J. Feldkamp, J. White, S. Hem, *J. Pharm. Sci.* 74 (1985) 478.
- [10] D. Lumsdon, L. Evans, *J. Colloid Interface Sci.* 164 (1994) 119.
- [11] P. Sipos, P. May, G. Hefter, *Analyst* 125 (2000) 955.
- [12] M. Bradbury, B. Baeyens, *Geochim. Cosmochim. Acta* 66 (2001) 2325.
- [13] L. Gorgeon, *Contribution à la modélisation physico-chimique de la rétention de radioéléments à vie longue par des matériaux argileux, Pierre et Marie Curie*, 1994.
- [14] R. Rundberg, Y. Albinsson, K. Vannerberg, *Radiochim. Acta* 66/67 (1994) 333.
- [15] R. De Levie, *How to Use Excel in Analytical Chemistry and in General Scientific Data Analysis*, Cambridge Univ. Press, 2001.
- [16] R. Kummert, W. Stumm, *J. Colloid Interface Sci.* 75 (1980) 373.
- [17] R. Kettler, D. Wesolowski, D. Palmer, *J. Chem. Eng. Data* 43 (1998) 337.
- [18] R. Mesmer, C. Patterson, R. Busey, H. Holmes, *J. Phys. Chem.* 93 (1989) 7483.
- [19] C. Patterson, G. Slocum, R. Busey, R. Mesmer, *Geochim. Cosmochim. Acta* 46 (1982) 1653.
- [20] C. Patterson, R. Busey, R. Mesmer, *J. Solution Chem.* 13 (1984) 647.